Proceedings of the Institute of Acoustics

STRUCTURAL INTENSITY IN SHELLS INCLUDING SHEAR EFFECTS

Krešimir TRDAK ; *CETIM - Département Acoustique, BP 67 - 60304 Senlis, France*

1. INTRODUCTION

Effects of the shear and the rotatory inertia on the dynamical behaviour of structures is a widely studied problem. Theories including these effects valid for beams and plates were derived respectively by Timoshenko [1] and Mindlin [2]. Shear effects in shells were studied by many authors. Soedel [3] has applied it on the vibrations of a cylindrical shell in order to explain the principle of the shear effect inclusion in shell theories of lower order. His model relies on Donnell theory. Shirakawa [4] did the same but reposing on Flügge theory. In the present paper, shear and rotatory inertia effects are added on Flügge theory and the newly created theory is referred as Flugge-Timoshenko theory. The paper studies influences of mentioned effects on the propagation of elastic waves in the cylindrical shell. Results for wavenumbers and intensities are presented graphically.

2. DISPERSION EQUATION

Application of the Timoshenko principle of the inclusion of shear effects in lower order theories for shells consists to take angles of section rotation as independant variables. The displacement field valid for wave motions in the cylindrical shell is therefore writen as

$$\{U\} = \begin{pmatrix} u(\xi,\eta,t) \\ v(\xi,\eta,t) \\ w(\xi,\eta,t) \\ \Theta_x(\xi,\eta,t) \\ \Theta_y(\xi,\eta,t) \end{pmatrix} = \begin{pmatrix} \hat{u}\cos(n\eta)e^{i(\chi\xi-\omega t-\pi/2)} \\ \hat{v}\sin(n\eta)e^{i(\chi\xi-\omega t)} \\ \hat{w}\cos(n\eta)e^{i(\chi\xi-\omega t)} \\ \hat{\Theta}_x\cos(n\eta)e^{i(\chi\xi-\omega t-\pi/2)} \\ \hat{\Theta}_y\sin(n\eta)e^{i(\chi\xi-\omega t)} \end{pmatrix} \quad , \tag{1}$$

where ξ and η denote non-dimensional coordinates along axial and circumferential direction of cylindrical shell while χ stands for the non-dimensional wavenumber in the shell

$$\xi = \frac{x}{a} \qquad \eta = \frac{y}{a} \qquad \chi = \frac{k_{sh}}{a} \quad . \tag{2}$$

Quantities u, v and w denote displacements in the axial, circumferential and lateral direction of the shell referent surface which is defined by the shell median radius a. Θ_x and Θ_y stand for angles of section rotation with the dimension of length

$$\Theta_x = \theta_x a \quad [m] \qquad \Theta_y = \theta_y a \quad [m] \quad , \tag{3}$$

which is done in order to simplify later calculations. Application of the matrix differential operator valid for a Flügge-Timoshenko theory on the displacement field (1) gives the equation of the dynamical equlibrium for a cylindrical shell

$$[L]\{\hat{U}\} = \{Q^{*m}\} \quad , \tag{4}$$

where components of the matrix $[L]$ are given by following expressions

$$
\begin{gathered}
L_{11} = \chi^2 + \frac{1-\nu}{2}(1+\beta^2)n^2 - \Omega^2 \qquad L_{12} = L_{21} = \frac{1+\nu}{2}\chi n \\
L_{13} = L_{31} = \nu\chi \qquad L_{14} = L_{41} = \beta^2\left(\chi^2 - \frac{1-\nu}{2}n^2 - \Omega^2\right) \\
L_{15} = L_{51} = 0 \qquad L_{22} = \frac{1-\nu}{2}\left[\chi^2 + \varsigma(1+\beta^2)\right] + (1+\beta^2)n^2 - \Omega^2 \\
L_{23} = L_{32} = \left[1 + \beta^2 + \varsigma\frac{1-\nu}{2}(1+\beta^2)\right]n \qquad L_{24} = L_{42} = 0 \\
L_{25} = L_{52} = \beta^2\left(\frac{1-\nu}{2}\chi^2 - n^2 - \Omega^2\right) - \varsigma\frac{1-\nu}{2}(1+\beta^2) \\
L_{33} = 1 + \beta^2 + \varsigma\frac{1-\nu}{2}\left[\chi^2 + (1+\beta^2)n^2\right] - \Omega^2 \qquad L_{34} = L_{43} = -\varsigma\frac{1-\nu}{2}\chi \\
L_{35} = L_{53} = -\left[\beta^2 + \varsigma\frac{1-\nu}{2}(1+\beta^2)\right]n \qquad L_{44} = \beta^2\left(\chi^2 + \frac{1-\nu}{2}n^2 - \Omega^2\right) + \varsigma\frac{1-\nu}{2} \\
L_{45} = L_{54} = \beta^2\frac{1+\nu}{2}n\chi \qquad L_{55} = \beta^2\left(n^2 + \frac{1-\nu}{2}\chi^2 - \Omega^2\right) + \varsigma\frac{1-\nu}{2}(1+\beta^2) \quad ,
\end{gathered}
\tag{5}
$$

with Ω and β^2 denoting non-dimensional frequency and shell thickness parameter respectively

$$
\Omega = \frac{a}{c_L}\omega \qquad c_L = \sqrt{\frac{E}{\rho(1-\nu)}} \qquad \beta^2 = \frac{h^2}{12a^2} \quad . \tag{6}
$$

Shear parameter ς is taken to be $5/6$ which is derived from the Donnell theory. In fact the estimation of the shear parameter is a great problem in the derivation of higher order flexural theories for shells. For example, Flügge theory describes fairly good curvature effects but it does not give explicit expressions for stresses. Donnell theory gives these expressions in the explicit form and the corresponding shear parameter equals $5/6$ which stands for both directions, axial and circumferential. In the reality, shear parameters for these directions should differ. In the equation (4) vectors $\{\hat{U}\}$ and $\{Q^{sm}\}$ denote vectors of complex displacement amplitudes and surface loads

$$
\{\hat{U}\} = \begin{pmatrix} \hat{u} \\ \hat{v} \\ \hat{w} \\ \hat{\Theta}_x \\ \hat{\Theta}_y \end{pmatrix} \qquad \{Q^{sm}\} = \frac{a^2}{C}\begin{pmatrix} 0 \\ 0 \\ q_n^{sm}(\xi,\eta,t) \\ 0 \\ 0 \end{pmatrix} \quad . \tag{7}
$$

The attention is here given exclusively to radial loads which is evident from the composition of the load vector $\{Q^{sm}\}$. For an empty shell this vector equals zero. If the shell is filled with an acoustic fluid the term $q_n^{sm}(\xi,\eta,t)$ reads [6]

$$
q_n^{sm}(\xi,\eta,t) = \left(1 - \frac{h}{2a}\right)F_{sf}\,\dot{w}\cos(n\eta)e^{i(\chi\eta-\omega t)} \qquad F_{sf} = \Omega^2\frac{\rho_f}{\rho_c}\frac{a}{h}\frac{1}{\kappa}\frac{J_n(\kappa)}{J_n'(\kappa)} \quad , \tag{8}
$$

where h is the shell thickness, ρ_f, ρ_c denote fluid and shell densities, $J_n(\kappa)$, $J_n'(\kappa)$ denote Bessel function of order n and its first derivative with respect of the non-dimensional radial wavenuber in fluid $\kappa = k_{fi}^r a$. Non-dimensional wavenumbers are related by the equation [6]

$$
\chi^2 + \kappa^2 = \left(\frac{c_L}{c_{fi}}\Omega\right)^2 \tag{9}
$$

with c_{fi} denoting the sound velocity in the fluid. One obtains wavenumbers in the shell and in the fluid as solutions of a dispersion equation for the shell which is

$$det([L]) = 0 \quad , \tag{10}$$

and the one for the fluid (9). The nature of Bessel functions obliges the usage of numerical procedures [9]. Insertion of calculated wavenumbers in the equation (4) gives displacement amplitude ratios

$$\Gamma_x = \frac{\hat{u}}{\hat{w}} \qquad \Gamma_y = \frac{\hat{v}}{\hat{w}} \qquad \Upsilon_x = \frac{\hat{\Theta}_x}{\hat{w}} \qquad \Upsilon_y = \frac{\hat{\Theta}_y}{\hat{w}} \tag{11}$$

which are used later in expressions for the structural intensity.

Expressions for the axial component of the structural intensity are given here in their final form, written in terms of displacements. Total intensity in the farfield of the cylindrical shell equals [7]

$$I_x = \frac{C}{a}(\ll \overline{\Lambda_m} \gg_0 + \ll \overline{\Lambda_f} \gg_0 + \ll \overline{\Lambda_c} \gg_0 + \tag{12}$$
$$+ \sum_{m=1}^{M} \sum_{n=1}^{N} \ll \overline{\Lambda_m} \gg_{n;m} + \ll \overline{\Lambda_f} \gg_{n;m} + \ll \overline{\Lambda_c} \gg_{n;m})$$

were $\ll\gg$ denotes space averaging, $\overline{\Lambda}_m$, $\overline{\Lambda}_f$, $\overline{\Lambda}_c$ denote contribution due to membranous, flexural and curvature effects in the shell. For circumferential modes superior or equal to 1, $n \geq 1$:

$$\ll \overline{\Lambda_m} \gg_{n;m} = \frac{\omega}{4}\Big[(\chi_{n;m}\Gamma^u_{n;m} + \nu)\Gamma^u_{n;m} + (\frac{1+\nu}{2} n \Gamma^u_{n;m} + \frac{1-\nu}{2}\chi_{n;m}\Gamma^v_{n;m})\Gamma^v_{n;m}\Big] D^w_{n;m} \tag{13}$$

$$\ll \overline{\Lambda_f} \gg_{n;m} = \beta^2 \frac{\omega}{4}\Big[(\varsigma\frac{1-\nu}{2} + \chi_{n;m}\Upsilon^x_{n;m})\Upsilon^x_{n;m} + (\frac{1+\nu}{2} n \Upsilon^x_{n;m} + \frac{1-\nu}{2}\chi_{n;m}\Upsilon^y_{n;m})\Upsilon^y_{n;m}\Big] D^w_{n;m} \tag{14}$$

$$\ll \overline{\Lambda_c} \gg_{n;m} = \beta^2 \frac{\omega}{2}\chi_{n;m}\Big(\Gamma^u_{n;m}\Upsilon^x_{n;m} + \frac{1-\nu}{2}\Gamma^v_{n;m}\Upsilon^y_{n;m} + \varsigma\frac{1-\nu}{4}\Big) D^w_{n;m} \quad . \tag{15}$$

Breathing mode represents a special case with torsional branches (denoted by the subscript "0;t" in expressions given bellow) uncoupled from other branches of the dispersion curve

$$\ll \overline{\Lambda_m} \gg_0 = \frac{\omega}{2}\sum_l \Big[(\chi_{0;l}\Gamma^u_{0;l} + \nu)\Gamma^u_{0;l} D^w_{n;m} + \sum_t \frac{1-\nu}{2}\chi_{0;t} D^v_{0;t} \tag{16}$$

$$\ll \overline{\Lambda_f} \gg_0 = \beta^2 \frac{\omega}{2}\Big[\sum_l (\chi_{0;l}\Upsilon^x_{0;l} + \varsigma\frac{1-\nu}{2})\Upsilon^x_{0;l} D^w_{0;l} + \sum_t \frac{1-\nu}{2}\chi_{0;t}\mathcal{D}^y_{0;t}\Big] \tag{17}$$

$$\ll \overline{\Lambda_c} \gg_0 = \beta^2 \omega\Big[\sum_l \chi_{0;l}(\Gamma^u_{0;l}\Upsilon^x_{0;l} + \varsigma\frac{1-\nu}{2}) D^w_{0;l} + \sum_t \frac{1-\nu}{2}\chi_{0;t} D^v_{0;t}\mathcal{D}^y_{0;t}\Big] \quad , \tag{18}$$

where

$$D^w_{n;m} = |\hat{w}^+|^2_{n;m} - |\hat{w}^-|^2_{n;m} \qquad D^w_{0;l} = |\hat{w}^+|^2_{0;l} - |\hat{w}^-|^2_{0;l} \tag{19}$$

$$D^v_{0;t} = |\hat{v}^+|^2_{0;t} - |\hat{v}^-|^2_{0;t} \qquad \mathcal{D}^y_{0;t} = |\hat{\Theta}_y{}^+|^2_{0;t} - |\hat{\Theta}_y{}^-|^2_{0;t} \qquad C = \frac{Eh}{1-\nu} \quad . \tag{20}$$

3. DISCUSSION OF RESULTS AND CONCLUSIONS

The Flügge-Timoshenko theory introduces two fundamental differences as regards to lower order theories. The first one is the existence of fifth branch of the dispersion curve for an empty shell and the second one is the existence of the cut-on frequency for each branch of the dispersion curve. One should keep in mind that dispersion curves for lower order theories possess four branches and that only three of them cut the frequency axe. These fundamental novelties are fairly well represented in the figure 1.
Other differences between results of presented theory and those of lower order are of purely numerical nature. All remarks given bellow are issued from the comparison between results given by Flügge (F) and Flügge-Timoshenko (F-T) theory valid for a circular stell shell of the thickness to radius ratio of 1/10.

1. **Cut-on frequencies:** For all branches of the dispersion curve for the empty shell, F-T cut-on frequencies are inferiour to those valid for F theory. The only exception is the cut-on frequency of the third branch for the breathing mode. Differences raise for higher circumferential modes and relative differences are much bigger for the first branch and the third branch when compared with the second one (for a given mode one branch is prior to some other if it cuts the frequency axe before that other branch).

2. **Wavenumbers:** The biggest divergences for wavenumbers are observed in narrow frequency intervals following cut-on frequencies, where the "fresh" real branch of the dispersion curve ascends very rapidly (see fig. 2). For the stabilized real branch, wavenumbers start to diverge more than 5[%] for wavelengths inferiour to the shell mean radius.

3. **Structural intensity:** The repartition of structural intensity in membranous, flexural and curvature contribution defined by Pavić in [7] facilitates the observation of a particular real branch of the dispersion curve. From figures 3. and 4. one can see that the structural intensity is either of dominantly membranous or flexural nature. Such a repartition stays the same for both theories. Notable differences between total values of structural intensity exist in the narrow frequency interval following the cut-on frequency of a particular branch, as it was already remarked for wavenumbers. In the frequency domain where the membranous component of the intensity is dominant, two theories give practically the same values. The situation changes radically for frequencies where the membranous contribution starts to descend abruptly. Relative differences of 5[%] appear already at wavelengths which equal triple mean shell radius. For wavelengths which equal the mean shell radius, F-T values of the structural intensity are almost 50 [%] lower than F values.

Two principal conclusions can be established from remarks given above. Firstly, Flügge-Timoshenko theory cancels the paradox of the purely imaginary branch existing in the high frequency domain, which is valid for lower order theories. Physically, the consequence is much better description of nearfield effects in the high frequency domain. Secondly, a domain of validity for lower order theories could be established. If the criterium of validity is the wavenumber than lower order theories are sufficiently precise for frequencies which do not pass beyond the limit frequency for which the corresponding wavelength of a particular real branch equals the mean radius of the cylindrical shell. The criterium of structural intensity is much more severe. The limit wavelength is here the one which equals triple mean radius of the cylindrical shell.

REFERENCES

[1] Timoshenko S.: "On the corrections for shear of the differential equations for transverse vibrations of prismatic bars", 1972 Philosophical Magazine 41, pp. 742—748

STRUCTURAL INTENSITY IN SHELLS INCLUDING SHEAR EFFECTS

[2] **Mindlin R. D.**: "Influence of rotatory inertia and shear on flexural motions of isotropic elastic plates", 1951 Journal of Applied Mechanics 18, pp. 31—38

[3] **Soedel W.**: "On the vibration of shells with Timoshenko-Mindlin type shear deflections and rotatory inertia", Joural of Sound and Vibration (1982), 83(1), pp. 67—79

[4] **Shirakawa K.**: "Effects of shear deformations and rotatory inertia on vibrations and buckling of cylindrical shells", Journal of Sound and Vibration (1983) 91(3), pp. 425—437

[5] **Fuller C. R.**: "The effects of wall discontinuities on the propagation of flexural waves in cylindrical shells", Journal of Sound and Vibration (1981) 75(2), pp. 207—228

[6] **Fuller C. R., Fahy F. J.**: "Characteristics of wave propagation and energy distributions in cylindrical elastic shells filled with fluid", Journal of Sound and Vibration (1982) 81(4), pp. 501—518

[7] **Pavić G.**: "Vibrational energy flow in elastic circular cylindrical shells", Journal of Sound and Vibration (1990) 142(2), pp. 293—310

[8] **Trdak K.**: "Intensite vibratoire dans les coques cylindriques vides", Rapport de stage pour l'obtention de DEA, CETIM 1991

[9] **Brazier-Smith P. R., Scott J. F. M.**: "On the determination of the roots of dispersion equations by use of winding number integrals", Journal of Sound and Vibration (1991) 145(3), pp. 503—510

FIGURES

Figures given bellow are valid for the steel shell of the thickness to mean radius ration of 1/10. All quantities represented by these diagrams are results of Flügge-Timoshenko theory. Figure 1 represents branches of the dispersion curve for the breathing mode ($n = 0$) valid for the empty shell. Five branches figure on the 3D diagram showing the dependance of the complex wavenumber of the non-dimensional frequency. Figure 2 represents branches of the dispersion curve for the mode $n = 1$ valid for the shell filled with water. Branches are presented in the 3D diagram whose axes are as those in figure 1: real and imaginary part of the wavenumber and the non-dimensional frequency. Figures 3 and 4 represent membranous and flexural contribution to the structural intensity in the farfield for the shell filled with water, for the circumferential mode $n = 1$. Both contributions are presented in 2D diagram where the horizontal axe represents non-dimensional frequency.

STRUCTURAL INTENSITY IN SHELLS INCLUDING SHEAR EFFECTS

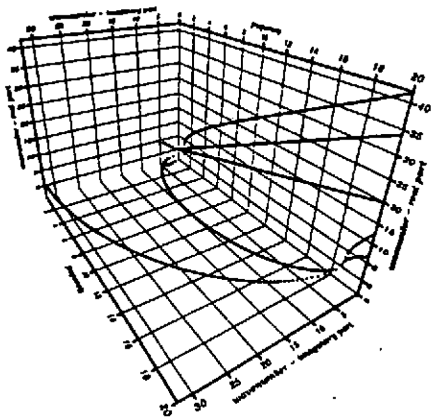

Fig. 1. *Dispersion curve, empty steel shell, mode n=0*

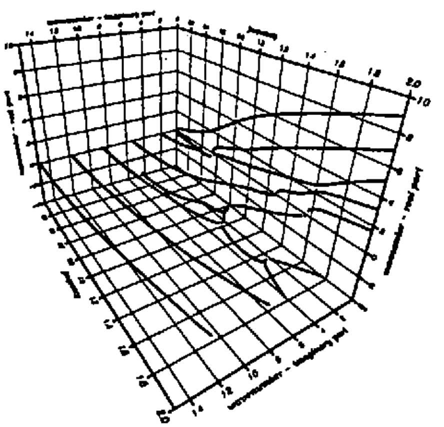

Fig. 2. *Dispersion curve, steel/water, mode n=1*

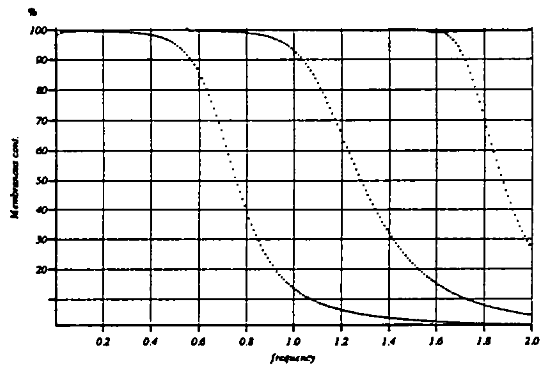

Fig. 3. *Membranous contribution, steel/water, mode n=1*

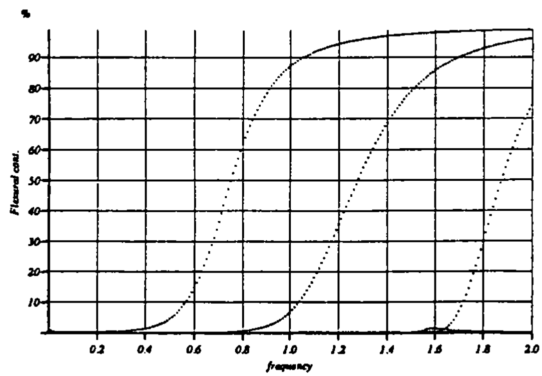

Fig. 4. *Flexural contribution, steel/water, mode n=1*